Article

On the Surface Quality of CFRTP/Steel Hybrid Structures Machined by AWJM

Fermin Bañon [1,*], **Bartolome Simonet** [2], **Alejandro Sambruno** [1], **Moises Batista** [1] **and Jorge Salguero** [1]

1   Faculty of Engineering, Mechanical Engineering and Industrial Design Department, University of Cadiz, Av. Universidad de Cadiz 10, Puerto Real, 11519 Cadiz, Spain; alejandro.sambruno@uca.es (A.S.); moises.batista@uca.es (M.B.); jorge.salguero@uca.es (J.S.)
2   Nanotures SL, C. Inteligencia 19, Tecnoparque Agroalimentario, Jerez de la Frontera, 11591 Cadiz, Spain; bartolome.simonet@nanotures.com
*   Correspondence: fermin.banon@uca.es; Tel.: +34-956-48-32-91

check for updates

Abstract: The joining of dissimilar materials in a hybrid structure is a line of research of great interest at present. Nevertheless, the machining of materials with different machinability requires specific processes capable of minimizing defectology in both materials and achieving a correct surface finish in terms of functional performance. In this article, abrasive water jet machining of a hybrid carbon fiber-reinforced thermoplastics (CFRTP)/Steel structure and the generated surface finish are studied. A parametric study in two stacking configurations (CFRTP/Steel and Steel/CFRTP) has been established in order to determine the range of cutting parameters that generates the lowest values in terms of arithmetic mean roughness (Ra) and maximum profile height (Rz). The percentage contribution of each cutting parameter has been identified through an ANOVA analysis for each material and stacking configuration. A combination of 420 MPa hydraulic pressure with an abrasive mass flow of 385 g/min and a travel speed of 50 mm/min offers the lowest Ra and Rz values in the CFRTP/Steel configuration. The stacking order is a determining factor, obtaining a better surface quality in a CFRTP/Steel stack. Finally, a series of contour diagrams relating surface quality to machining conditions have been obtained.

Keywords: AWJM (abrasive water jet machining); CFRTP (carbon fiber-reinforced thermoplastics); hybrid structure; surface quality; Ra; Rz; C/TPU (carbon/thermoplastic polyurethane)

1. Introduction

Carbon fiber-reinforced thermoplastics (CFRTP) composites have an excellent weight-to-mechanical property ratio and high impact and corrosion resistance [1]. These are very interesting materials due to their ability to be remolded after curing, adopting new geometries and being of great interest for mass production [2]. Applications such as chassis in the automotive sector or the development of a lighter fuselage with better fatigue resistance developed by the company STELIA are an example of the current interest in these materials. In addition, in comparison with thermosets (CFRP), they have shorter production times and the possibility of storing the matrix at room temperature which reduces the final costs [3]. Within the wide range of thermoplastic polymers, thermoplastic polyurethane (TPU) can achieve high performance in service. The shaping of this matrix together with carbon fibers results in a flexible compound that can be adapted to various uses [4].

In order to increase the performance of these materials, current research is focused on their bonding with metal alloys in the form of hybrid structures through laser welding or friction stir welding processes [5]. These materials are essential elements in structural applications in the industry nowadays

due to their mechanical properties, lightness, and corrosion resistance. Nevertheless, they must be joined to metallic elements to obtain a more robust structure that combines the performance of both materials in the form of a hybrid design [6]. Furthermore, in terms of production, the manufacture and subsequent machining of both materials at the same time means a reduction in operating times. A kind of hybrid structure of great interest is the union of CFRTP with a steel in order to obtain a structural element of high performance. This turns them into elements of great interest for the automotive sector where weight reduction is required and, at the same time, their ability to produce them in mass [2,7].

Their combination with a structural steel allows to obtain a hybrid structure of excellent performance and lightness minimizing energy consumption and CO_2 emissions. Nevertheless, the quality of the interlayer of these materials on applying an adhesive or thermal bonding process has been studied due to the formation of thermal defects or the formation of bubbles due to poor surface preparation of the steel [8,9]. In addition, according to the selected process, the thermoplastic matrix of the CFRTP can be used as an integrating element of the hybrid structure affecting the final thickness [10].

In addition, to achieve a final geometry, specific machining processes are required due to the anisotropic behavior of these materials, as well as the low glass transition temperature of some thermoplastics [11]. Inside conventional processes, such as drilling or milling, wear caused to the cutting edges increases the final costs and reduces the efficiency of these processes. Processes such as milling generate a smooth and clean surface with Rz values close to 9 μm and Ra values close to 2 μm [12,13]. This is in line with the results obtained in the conventional machining of thermoset composite materials, where results below 3.2 μm are required due to aeronautical tolerances [14].

Nevertheless, although very low values are obtained, the machining temperatures deteriorate the thermoplastic matrix and cause delaminations in regions in which the reinforcement is left unprotected [12]. In addition, the fact of machining two materials of different machinability requires the use of specific cutting geometries and complex machining strategies with change of cutting parameters in the interlayer. This means an increase in operating time and costs.

On the contrary, within nonconventional technologies, abrasive water jet machining (AWJM) has proved to be a very effective technology for machining this type of material [13,15,16]. It is a flexible process, capable of achieving high material removal rates and low cutting forces and machining different materials at the same time. In addition, due to the nature of the cutting process, the temperatures reached are very low, which minimizes thermal defects [17]. Furthermore, it is a clean and environmentally friendly technology, a fundamental aspect within the field of "Green machining," and does not generate suspended particles that could affect the health of the operators. This technology offers advantages such as the recovery of abrasive particles after machining, which can be reused after treatment, and no harmful gases are generated [18]. Another important point is the retention of particles of the machined material in the pool pit, especially in composite materials, preventing them from remaining in suspension, avoiding the exposure of the operators to a harmful atmosphere. The cutting tool is water, which can be reused after machining, and abrasive particles, which can be recovered later and treated to be reused.

Nevertheless, there is little literature on abrasive water jet machining of dissimilar material stacks. Most focus on machining FMLs or CFRP/Titanium stacks due to their relevance within the aeronautical industry [19–23]. These studies are focused on the influence of the parameters that govern abrasive water jet machining on the surface quality generated, as well as on the defectology associated with this process such as the taper angle. Although there is literature on water jet machining of thermoplastic composites [24] and steel alloy [25], little information exists on machining these materials in the form of a hybrid structure.

A crucial aspect in the machining processes is the surface quality obtained. The divergence of the water jet during machining generates a reduction in the kinetic energy that results in regions of different surface quality. Thus, in the initial moments of machining, the overlapping of the abrasive particles generates a highly eroded zone known as IDR (initial damage region) [26]. Subsequently,

the convergence of the jet generates a stable zone in which a homogeneous surface is obtained, known as the SCR (smooth cutting region) [27]. Finally, due to the reduction of the kinetic energy and cutting capacity of the water jet, the surface generated has a region with very high irregularities in the form of grooves known as RCR (rough cutting region) [28,29].

In this sense, the stacking order of the hybrid structure has a fundamental role to play in the development of these regions. Depending on which material receives the first impact of the water jet, the final quality obtained in the second material will be conditioned by the difference in its machinability [23].

For this reason, minimizing water jet divergence during machining is a key aspect for achieving an acceptable surface quality. Thus, the correct selection of cutting parameters according to the order of stacking is essential to achieve this objective [30]. In studies carried out, the difference in results obtained between the composite material and the metal alloy when they are machined is also highlighted. This is due to the fact that the composite material is anisotropic and the water jet is able to eliminate the matrix generating greater irregularities or the formation of delaminations. In contrast, the isotropy of the metal alloy allows a more stable and smoother cut, but is more affected by the effect of the abrasive particles in the initial zone (IDR).

Within the cutting parameters, traverse speed and hydraulic pressure seem to be the most relevant [31]. Increases in traverse speed lead to increased water jet divergence, especially in the second material, significantly raising the roughness in the material [25]. Pahuja et al. [30] also explains the importance of traverse speed in water jet machining of a hybrid CFRP/Ti structure. Here, by increasing the speed from 1 to 10 mm/min, the Ra values increase by 14% for the titanium alloy and 260% for the composite material. On the other hand, an increase in hydraulic pressure increases the jet's machining capacity, allowing for an improvement in surface quality and obtaining *Ra* values that are very close to each other [22].

Nevertheless, the combination of the different machinability between materials, their stacking order, and the lack of knowledge about a range of cutting parameters capable of machining this type of hybrid structures require further studies. Due to this, this article proposes a parametric study in abrasive water jet machining of a hybrid CFRTP/Steel structure. The surface quality in terms of *Ra* and *Rz* has been evaluated in each material for the two stacking configurations (CFRTP/Steel and Steel/CFRTP). The difference in results between the two configurations has been evaluated, as well as a range of cutting parameters that improve surface quality has been determined. The machining of dissimilar materials in the form of a hybrid structure generates a difference in surface quality between the two elements that must be minimized or eliminated. Nevertheless, the study of the surface quality in both materials separately has been the main objective of this work. Thus, a range of cutting parameters that improves the surface quality has been determined. In order to obtain a homogeneous cut, a ratio between the results obtained for the composite material and the metal alloy has been established to identify which variation in cutting parameters generates the greatest difference in surface quality. Finally, an ANOVA analysis and a set of contour diagrams using predictive mathematical models have been obtained for the most relevant roughness parameter.

2. Methodology

2.1. Materials

This article focuses on the machining of a hybrid structure in order to evaluate the surface quality obtained. The materials selected to obtain this structure were a thermoplastic composite material reinforced with carbon fiber (Twill 200 g/m^2) and a steel alloy S275. The main characteristics of the composite material are shown in Table 1. Reinforced thermoplastic laminates were produced by hot compression molding.

The CFRTP used has a thermoplastic polyurethane matrix with a melting temperature of 145° and the final thickness of 2.1 mm and is composed of 7 layers in 0° and 90° orientations.

Table 1. Mechanical properties of thermoplastic composite material (carbon fiber-reinforced thermoplastics, CFRTP).

Tensile Strength (MPa)	Tensile Modulus (GPa)	Flexural Strength (MPa)	Flexural Modulus (GPa)	Compression Strength (MPa)	ILSS (MPa)
749	27.8	640	8.4	136	9.8

On the other hand, the thickness of the steel was 3 mm, obtaining a final thickness of the hybrid structure of 5.1 mm. This carbon steel is a structural type with wide applications in the industrial sector due to its mechanical properties, and it is of great interest to combine it with a composite material in order to obtain a hybrid structure. Its main characteristics are shown in Table 2.

Table 2. Characteristics of S275 steel.

%C	%Fe	%Mn	%P	%S	%Si	Yield Strength (MPa)	Tensile Strength (MPa)
0.25	98.01	1.60	0.04	0.05	0.05	275	450

The bonding between these materials was carried out by thermoforming in a hot plate press with the aim of obtaining a continuous and quality bond to avoid the formation of delaminations in the interlayer and to relate possible defects to the machining conditions. The characteristics of the thermoplastic matrix allow the matrix itself to be used as an integrating element between both materials by changing from a solid to a liquid state when its glass transition temperature is exceeded. Subsequently, the matrix expands and impregnates the surface of the steel alloy to generate a constant bond after it has cooled down. To ensure a quality bond, the steel surface is modified by sand-blasting, using a pressure of 5 bar, 630 μm corundum particles, and an impact distance of 100 mm. Because of it, a surface free energy value of 50 mJ/m^2 [32] was obtained.

2.2. Abrasive Water Jet Machining (AWJM)

The equipment used consisted of a water jet cutting machine (TCI Cutting, BP-C 3020, Valencia, Spain). The nozzle of the machine had a diameter of 0.8 mm, an orifice diameter of 0.3 mm, and a nozzle length of 94.7 mm. The AWJM machine was equipped with an ultrahigh capacity pump (KMT, 158 Streamline PRO-2 60, Bad Nauheim, Germany). All trials were carried out by 120 mesh Indian Garnet abrasive particles.

Three cutting parameters were modified according to the literature consulted. Three levels of hydraulic pressure (P), traverse speed (TS), and abrasive mass flow (AMF) were established (Table 3). At the same time, in order to obtain a greater robustness and repeatability in the results obtained, each combination of cutting parameters were carried out twice, obtaining a total of 54 tests. Due to its importance in the conservation of kinetic energy of the water jet, the jet-piece distance was set at 3 mm.

Table 3. Cutting parameters for abrasive water jet texturing.

Hydraulic Pressure—P (MPa)	Abrasive Mass Flow—AMF (g/min)	Traverse Speed—TS (mm/min)
250, 340, 420	225, 340, 385	50, 100, 300

The tests consisted of slots with a machining length of 30 mm and a gap between cuts of 6 mm. In order to guarantee a constant flow and traverse speed, the cuts were started 15 mm before the beginning of the material (Figure 1).

On the other hand, the order of the materials during machining is a key parameter in the final quality. Because of this, each test has been performed in two stacking configurations, CFRTP/Steel, and Steel/CFRTP.

Figure 1. Abrasive water jet machining of a hybrid structure Steel/carbon fiber-reinforced thermoplastics (CFRTP).

2.3. Surface Quality Evaluation

The surface finish after machining processes is a key parameter in determining the functional performance of the geometry obtained. The importance of the surface of the parts in the functional behavior of the latter is relevant when considering that it is through their surfaces that contact is established between them, being the main basis of most mechanical functions [33].

Surface quality in abrasive water jet machining is a key factor. The loss of kinetic energy of the water jet in combination with poor selection of cutting parameters produces large variations. This results in a first region that is highly affected by abrasive particles and a final zone of high roughness due to the formation of grooves. This in combination with the fact that dissimilar materials are being machined at the same time makes it an essential parameter to study.

Due to this, the surface quality has been evaluated in terms of arithmetic mean roughness (*Ra*) and maximum profile height (*Rz*). The anisotropy of the composite material and the possible formation of defectology associated with the loss of thermoplastic matrix requires the study of several parameters that provide more complete and real information about the surface obtained [34]. Three measurements were made at three height levels in each material (Figure 2). Each roughness profile was measured at three different levels, i.e., at 25%, 50%, and 75% of the thickness of each material. The goal was to determine the presence of the three characteristic regions in abrasive water jet machining in terms of surface quality: IDR (initial damage region), SCR (smooth cutting region), and RCR (rough cutting region). The measurements were made in a perpendicular direction to the grooves generated by the water jet.
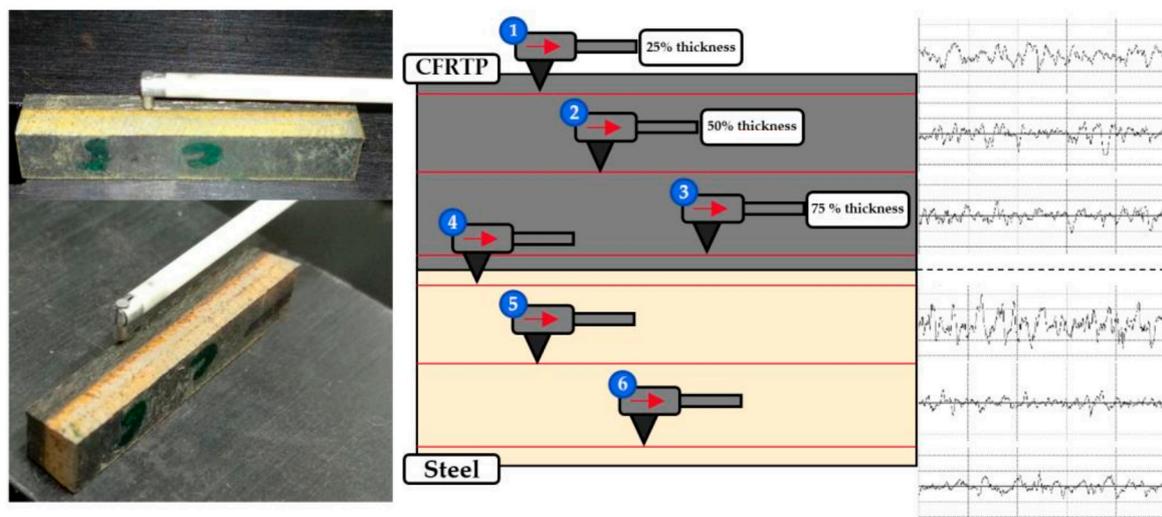

Figure 2. Graphical representation of surface quality evaluation.

A roughness-meter (Mahr Perthometer PGK 120, Göttingen, Germany) was used. The surface quality evaluation was carried out following ISO 4288:1999 standard. A cut-off of 2.5 mm was established for a total evaluation length of 12.25 mm. Stylus with 2 µm tip radius and 90° tip angle was used for the measurements, reference M-250 from Mahr.

Finally, the surface generated after the surface modification was evaluated by visual inspection using a scanning electron microscope (Hitachi, VP-SEM SU1510, Schaumburg, IL, USA).

3. Results and Discussion

3.1. CFRTP/Steel

This section shows the results obtained in the first CFRTP/Steel configuration in order to determine the influence of the cutting parameters. The surface quality obtained in the thermoplastic composite material in terms of Ra is shown in Figure 3. For pressures of 250 MPa, two tendencies are observed when increasing the abrasive flow. When the traverse speed is 50 mm/min, high values of abrasive increase the roughness. This may be due to an excess amount of particles impacting the surface. In combination with reduced pressure, the jet does not have enough energy to obtain a clean cut (Figure 4). Thus, the intercollisions of the abrasive particles reduce its cutting capacity, producing a more eroded zone [35].
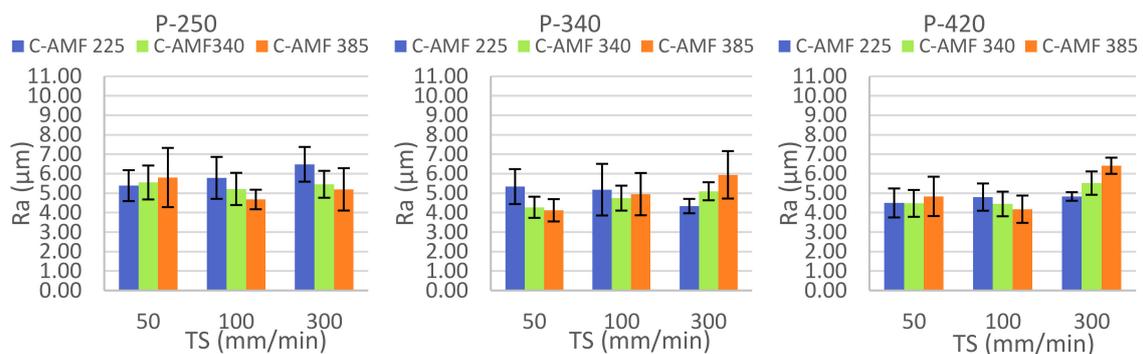
Figure 3. CFRTP surface quality results in terms of arithmetic mean roughness (*Ra*) as a function of the cut-off parameters set for the CFRTP/Steel configuration.
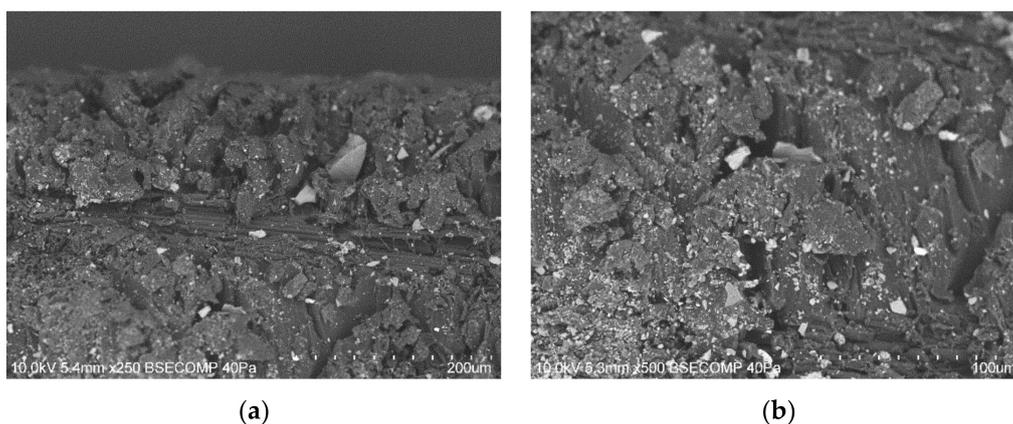

(**a**)　　　　　　　　　　　　　　　　　　　(**b**)

Figure 4. Initial damaged region (IDR) due to the erosive effect of the abrasive particles (hydraulic pressure (P) 250 MPa, traverse speed (TS) 300 mm/min, and abrasive mass flow (AMF) 385 g/min) at: (**a**) 250× and (**b**) 500×.

On the other hand, when the traverse speed increases its value, this trend for a hydraulic pressure of 250 MPa is totally opposite due to the increase in the kinetic energy of the water jet. This produces a rougher RCR zone due to the curvature of the water jet due to the loss of kinetic energy [36].

Nevertheless, as hydraulic pressure increases, the surface quality is directly influenced by the traverse speed, especially for pressures of 420 MPa.

Thus, an increase in pressure and abrasive flow at reduced traverse speeds produces a stable water jet capable of homogeneously machining all composite material [37].

When the traverse speed is maximum, the increase in pressure has a varying effect depending on the amount of abrasive particles applied in the machining. With a minimum flow rate of 225 g/min, there is a significant increase in the machining capacity of the water jet, obtaining a more constant material removal and reducing the *Ra* values from 7 to almost 5 μm.

The increase of the abrasive particles improves the cutting capacity of the jet allowing a smoother region. This can be seen in the pressure of 250 MPa. However, a combination of high values of both hydraulic pressure and abrasive flow can be excessive resulting in a deterioration in surface quality. This may be due mainly to an excess of abrasive particles that intercollide, minimizing their erosive effect. In turn, this produces an increase in the IDR region increasing the abrasive particles adhered in the initial moments of machining and increasing the average roughness [15]. This in combination with the divergence between the inlet and outlet zones of the water jet due to a very high travel speed results in these variations when hydraulic pressure is increased.

Also, an increased pressure leads to a greater offset between the inlet area of the water jet and the outlet area. During this time, the kinetic energy of the water jet allowing the material to be machined is reduced. Thus, the impacts generated on the surface are more abrupt, generating irregularly shaped machined areas [26]. This could produce an area of higher roughness and poorer surface quality (Figure 5). These roughness profiles were made at three different levels as shown in Figure 2. The first profile at a distance equivalent to 25% of the thickness, the second profile at 50% of the thickness, and the third profile at 75% of the thickness of the material were obtained.
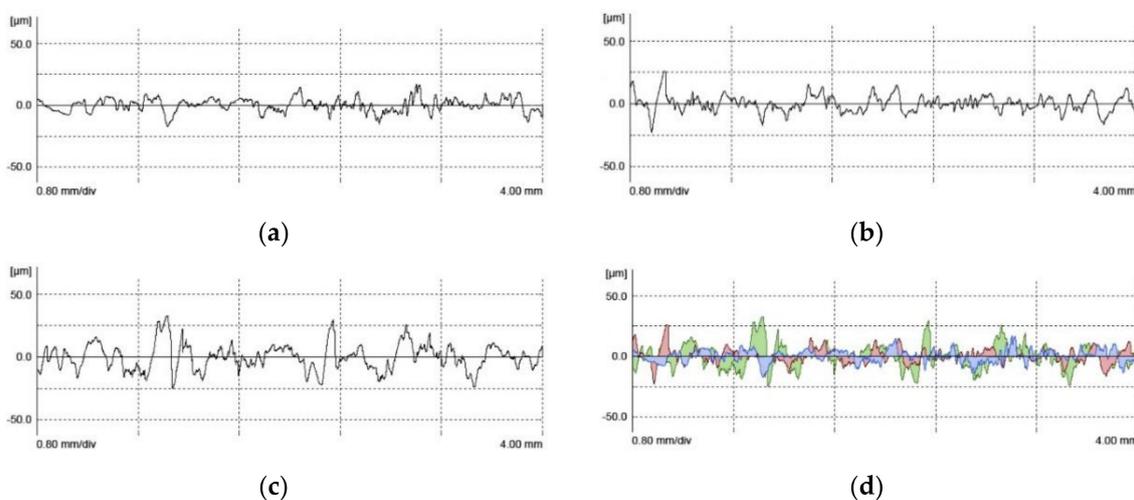

Figure 5. Roughness profiles for the combination of *P* of 420 MPa, *TS* of 300 mm/min, and *AMF* of 225 g/min for: (**a**) IDR, (**b**) smooth cutting region (SCR), (**c**) rough cutting region (RCR) region, and (**d**) overlapping roughness profiles.

This is corroborated by the results obtained for the parameter *Rz* (Figure 6). The trends obtained are very close to those obtained for Ra, which would justify the previously described trends. Thus, it can be seen that a combination of a pressure of 420 MPa, an abrasive flow of 385 g/min, and a traverse speed of 100 mm/min generate the minimum values of *Ra* and *Rz*.
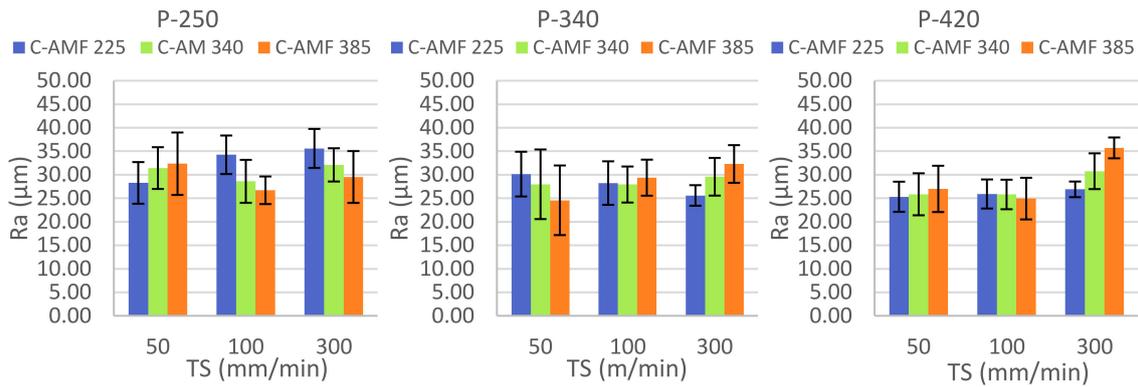
Figure 6. Maximum profile height (*Rz*) values for CFRTP in CFRTP/Steel configuration.

In addition, the surface quality of the steel in terms of Ra is shown in Figure 7 and in terms of Rz in Figure 8. It can be seen that lower values are obtained in the metal alloy compared to the composite material. This is due to the composition of both materials. The anisotropy of the composite material causes each layer to behave differently when interacting with the water jet [30].
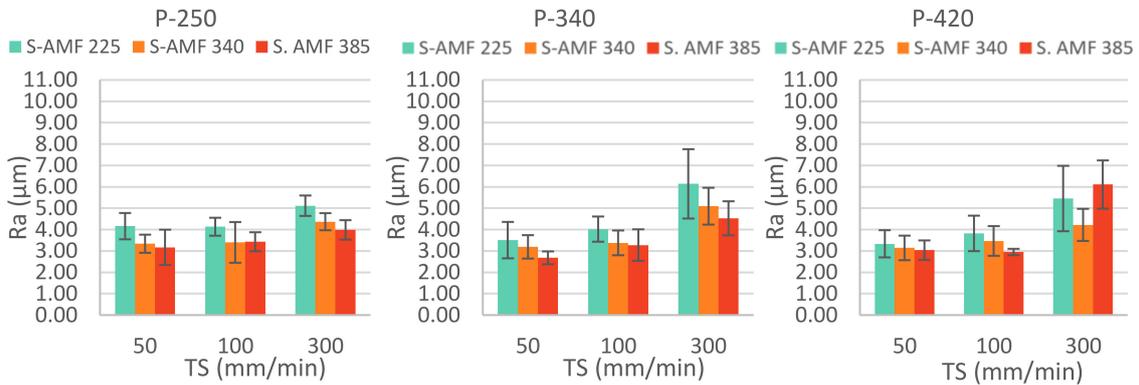

Figure 7. Steel surface quality results in terms of *Ra* as a function of the cut-off parameters set for the CFRTP/Steel configuration.
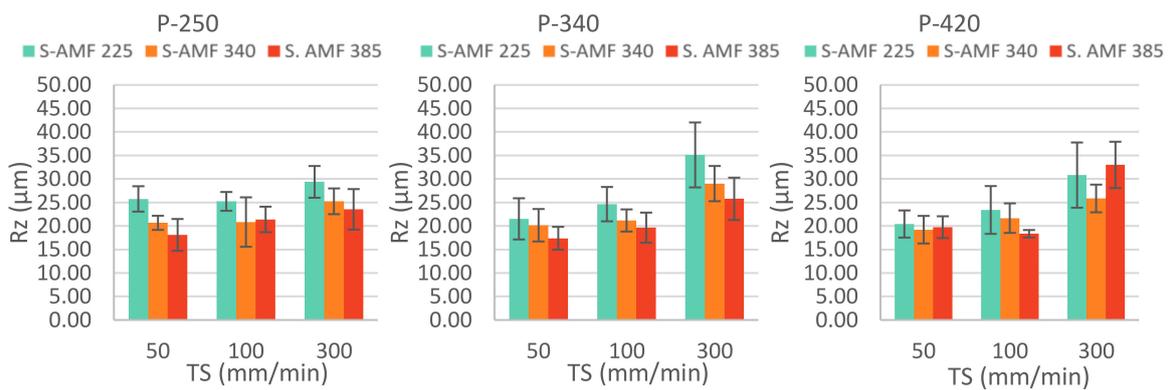
Figure 8. *Rz* values for steel in CFRTP/Steel configuration.

Furthermore, the different machinability of the reinforcement and matrix in combination with the dispersion of the water jet produces an effect known as hydrodistortion [21] (Figure 9). In addition, the main removal mechanism in the composite material was by microbending and fracture and in the matrix was by erosion. This results in a transversal removal of the matrix, leaving the reinforcement unprotected and generating a worsening of the surface quality (Figure 10).

Due to the monolithic composition of the steel, a more homogeneous machining has been obtained. This produces a smoother surface compared to composite material. However, as the second material is machined in the CFRTP/Steel configuration, a reverse situation is generated. A combination of a *TS* of 300 mm/min and an *AMF* of 340 g/min shows this effect. The divergence of the water jet between the inlet and outlet region is very high due to the destabilization of the water jet at this travel speed. This is enhanced by the difference in machinability between the two materials. In other words, the water jet is not capable of machining both materials consistently at the same time.

In addition, the reduced amount of abrasive particles minimizes the actual machinability of the water jet, resulting in a rougher surface [22].
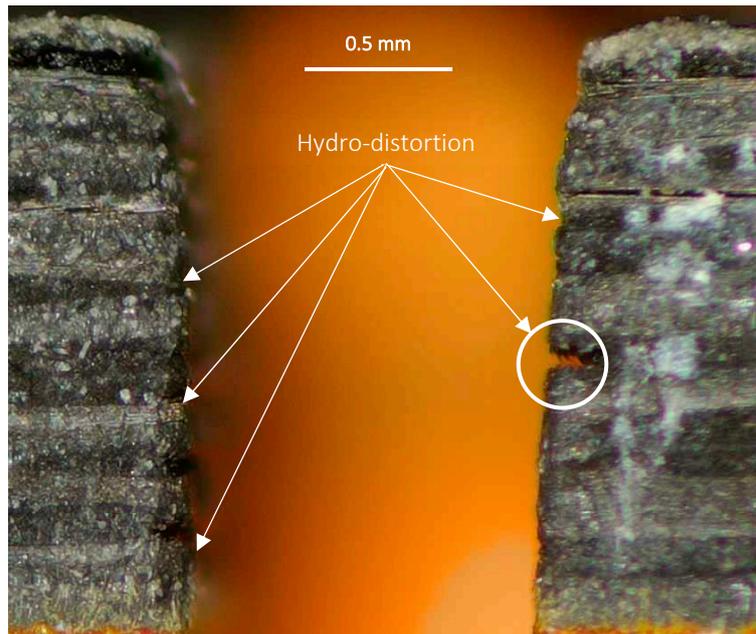
Figure 9. Hydrodistortion defect at a pressure of 250 MPa, an abrasive mass flow of 225 g/min, and a travel speed of 50 mm/min.
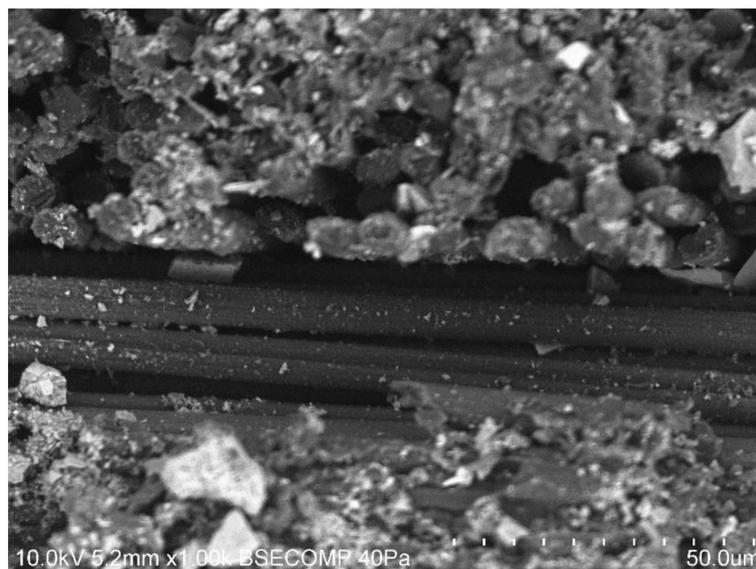

Figure 10. Loss of thermoplastic matrix leaving the reinforcement unprotected at 1000× (*P* of 250 MPa, *TS* of 300 mm/min, and *AMF* of 385 g/min).

Due to the low machinability of steel, the increased abrasive mass flow has a positive effect on the surface quality. An increase in particles enhances the erosive capacity of the water jet allowing it to penetrate the steel more easily due to greater stabilization in the cut [38]. This can be seen in most tests where an increase in this parameter generates a reduction in both *Ra* and *Rz*.

The trend of each cutting parameter in the surface quality generated in terms of Ra for each material is shown in Figure 11. In terms of hydraulic pressure, steel is the most important material as it is more difficult to machine and is the second material in the structure. An increase in this parameter improves the penetration capacity of the water jet, facilitating shear impacts on the surface and obtaining a better surface quality. An increase in the amount of abrasive particles reduces the resistance of the material when machined.

Nevertheless, depending on the level of pressure and traverse speed, it can become a negative aspect. On the contrary, the traverse speed seems to be the most critical parameter for surface quality. The increase from 50 to 300 mm/min produces a 40% increase in both materials due to the destabilization of the water jet and the inability to machine both materials at the same time.
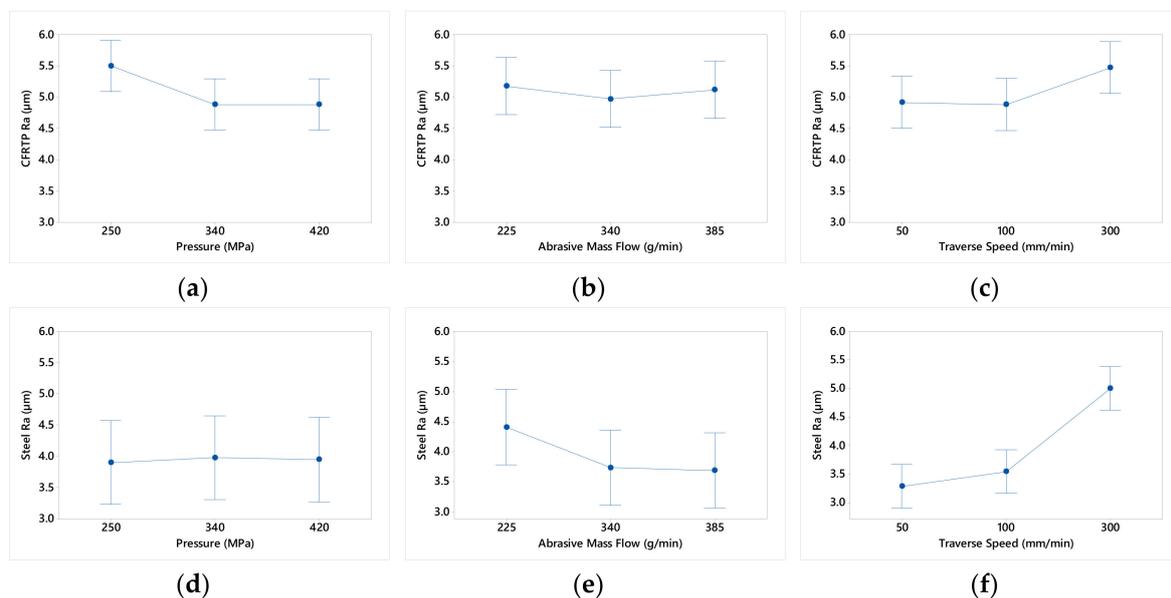

Figure 11. Cutting parameter trends in surface quality (*Ra*) in CFRTP/Steel configuration. (**a**) CFRTP Ra in function of *P*, (**b**) CFRTP Ra in function of *AMF*, (**c**) CFRTP Ra in function of *TS*, (**d**) Steel Ra in function of *P*, (**e**) Steel Ra in function of *AMF*, and (**f**) Steel Ra in function of *TS*.

3.2. Steel/CFRTP

The results obtained in the reverse stacking order for the composite material are shown in Figures 12 and 13.

Compared to the CFRTP/Steel configuration, the results obtained are slightly higher. This may be due to the positioning within the hybrid structure. When machining the metal alloy, a large part of the kinetic energy of the water jet is absorbed by this material, reducing the ability to penetrate the composite material [22,26]. This is especially outstanding when the pressure is minimal (250 MPa) and the amount of abrasive particles is insufficient. This produces an increase in the hydrodistortion effect between reinforcement and matrix resulting in a very rough surface where the reinforcement is not properly machined, generating high deviations (Figure 14).
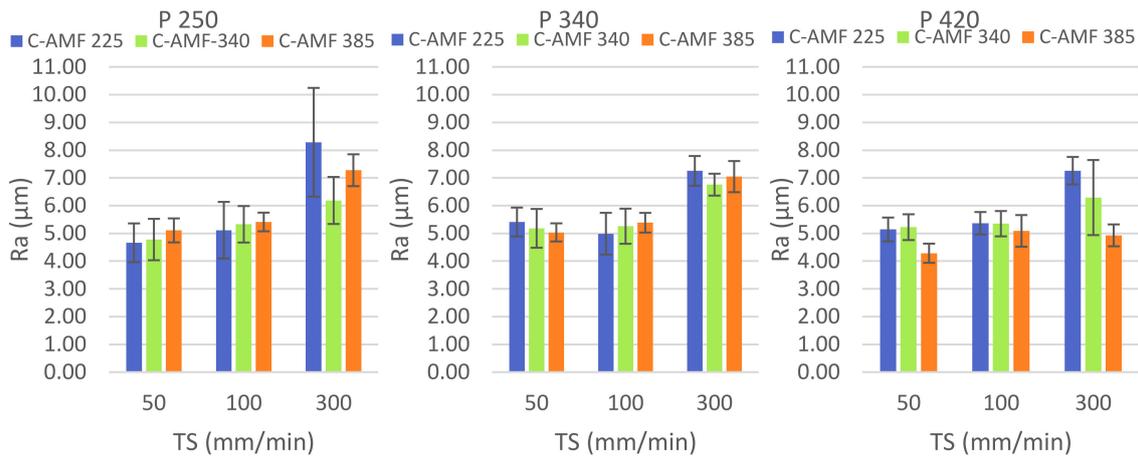
Figure 12. CFRTP surface quality results in terms of *Ra* as a function of the cutting parameters set for the inverse Steel/CFRTP configuration.
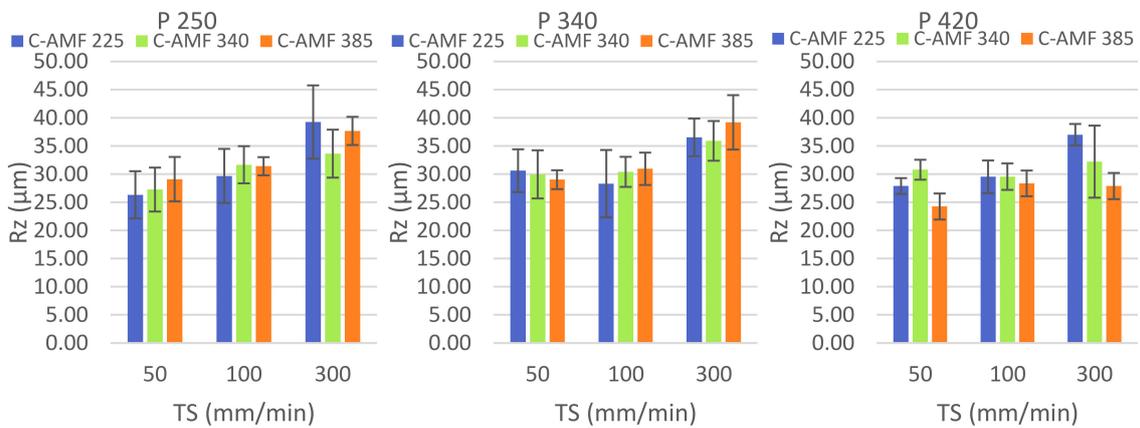

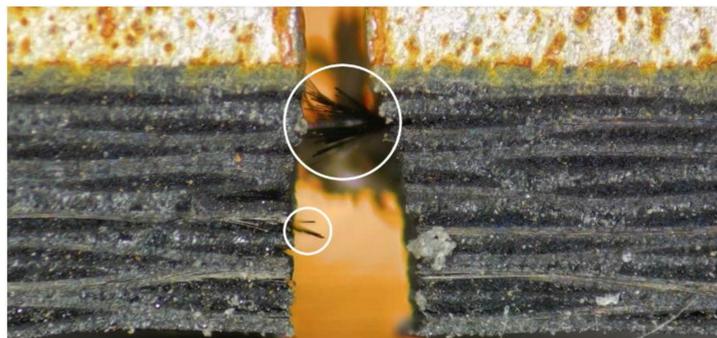**Figure 13.** *Rz* values for CFRTP in Steel/CFRTP configuration.

Figure 14. Reinforcements that are not machined, resulting in a worse surface quality.

The formation of a turbulent jet in the interlayer and the consequent loss of power of the water jet results in an unstable flow that generates a very rough area. This, in combination with the low cohesion between the reinforcement and the thermoplastic matrix, generates a separation between both leaving the reinforcement unprotected and increasing the final roughness [39]. This can be seen in Figure 15.

Again, similar trends are observed in both *Ra* and *Rz*. However, in contrast to the CFRTP/Steel configuration, both hydraulic pressure and abrasive mass flow do not seem to have such a significant effect on surface quality. Only when the speed is maximum, an increase in these parameters generates a noticeable difference. In the CFRTP/Steel configuration, the influence of these parameters is more noticeable because the water jet dispersion is lower. In this sense, the increase in pressure minimizes

the hydrodistortion defect in the composite material, minimizing the loss of kinetic energy prior to steel machining.

Thus, the machining capacity of the water jet is more constant and a variation in these parameters is more relevant. On the contrary, when the first material to be machined is steel, this energy loss is greater because it presents a greater difficulty to be machined, minimizing the effect of the cutting parameters in the composite material.

In contrast, the travel speed seems to have a more prominent effect in this configuration due to the dispersion of the water jet. When the jet starts machining at a very high speed and the first material (Steel) has a worse machinability, an excessive delay is generated between the machining of this and the second material (CFRTP) and an increase in the hydraulic pressure enhances the penetration capacity of the water jet improving the surface integrity in spite of obtaining very high *Ra* values [13].
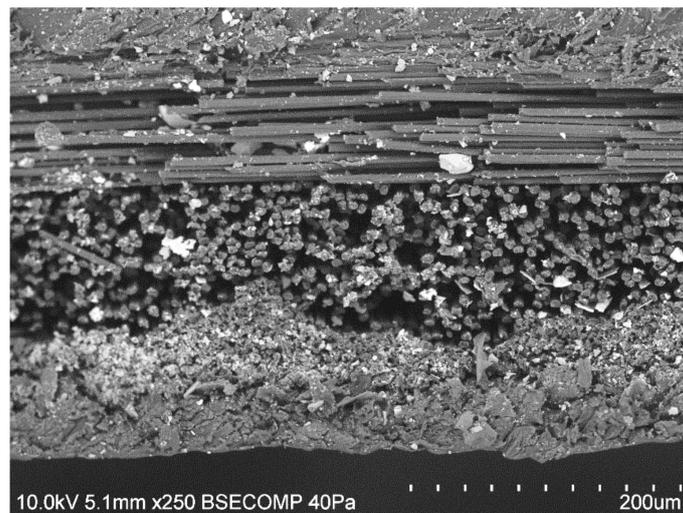

10.0kV 5.1mm x250 BSECOMP 40Pa   200um

Figure 15. Total loss of thermoplastic matrix leaving the reinforcement unprotected in 0° and 90° stacking orientation at 250× (*P* of 250 MPa, *TS* of 300 mm/min, and *AMF* of 385 g/min).

On the other hand, the results obtained in steel machining in terms of *Ra* (Figure 16) and *Rz* (Figure 17) are very close to those obtained in the reverse configuration. This would indicate that steel is the most decisive material in the machining of this structure. In terms of surface quality, the positioning of the steel does not affect the results obtained, but it does directly affect the final quality generated in the composite material.
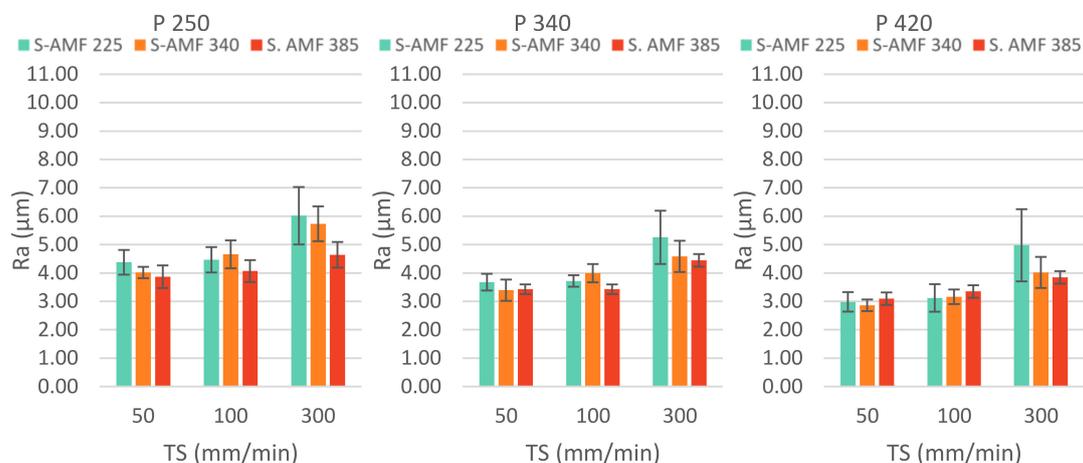

Figure 16. Steel surface quality results in terms of *Ra* as a function of the cutting parameters set for the inverse Steel/CFRTP configuration.

The three cutting parameters generate an improvement in the quality obtained. When the traverse speed is between 50 and 100 mm/min, it seems that the most dominant parameter is the hydraulic pressure by reducing the Ra values from 4 to 3 μm and minimizing the deviations obtained, which would indicate that the surface is very homogeneous. This is corroborated by the *Rz* results, which would indicate that the surface is smooth with constant surface variations. On the other hand, as with the other results, the increase at a speed of 300 mm/min significantly worsens the surface quality due to the destabilization of the water jet, which leads to an increase in the lag defect in the RCR region.

With regard to the abrasive flow, its effect is more noticeable when the speed is higher than 300 mm/min due to the loss of kinetic energy. An increase in this parameter improves the tearing of the steel by shear forces. In addition, flows of 385 g/min offer a very reduced deviation in both Ra and *Rz*, which would indicate minimal variations in the surface obtained. Thus, for this level of abrasive mass flow and a pressure of 420 MPa, very close surface quality values are obtained for speeds of 100 and 300 mm/min, allowing an increase in productivity in the machining of hybrid structures.
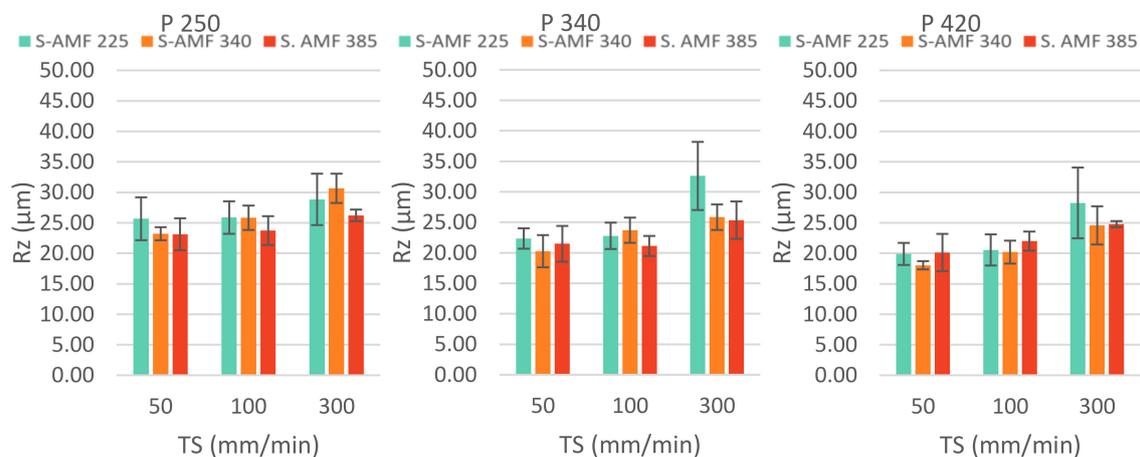

Figure 17. *Rz* values for steel in the Steel/CFRTP configuration.

The trends for each cutting parameter are shown in Figure 18. A great influence is observed on the composite material by increasing the hydraulic pressure and traverse speed. Being the second material to be machined in this stack directly affects the results obtained. Steel has a higher resistance to be machined and makes it difficult to stabilize the water jet prior to the machining of the composite material. This, in combination with the turbulence that can be generated in the interlayer, affects the surface quality by varying these parameters.

On the contrary, different trends have been observed in the surface quality of the steel compared to the CFRTP/Steel configuration. Thus, the pressure does not produce a significant variation in the results and the abrasive flow seems to slightly reduce Ra values that improves the surface quality. However, the trend of the traverse speed is constant and similar in both materials and stacking configurations with an increase in the results due to the delay in the water jet and not using the same amount of particles per unit area.

The machining of materials of different machinability reflects that the surface quality can be very disparate and that the machined part does not fulfill its function. The ratio between the Ra values for the CFRTP/Steel configuration is shown in Figure 19 and for the Steel/CFRTP configuration in Figure 20.
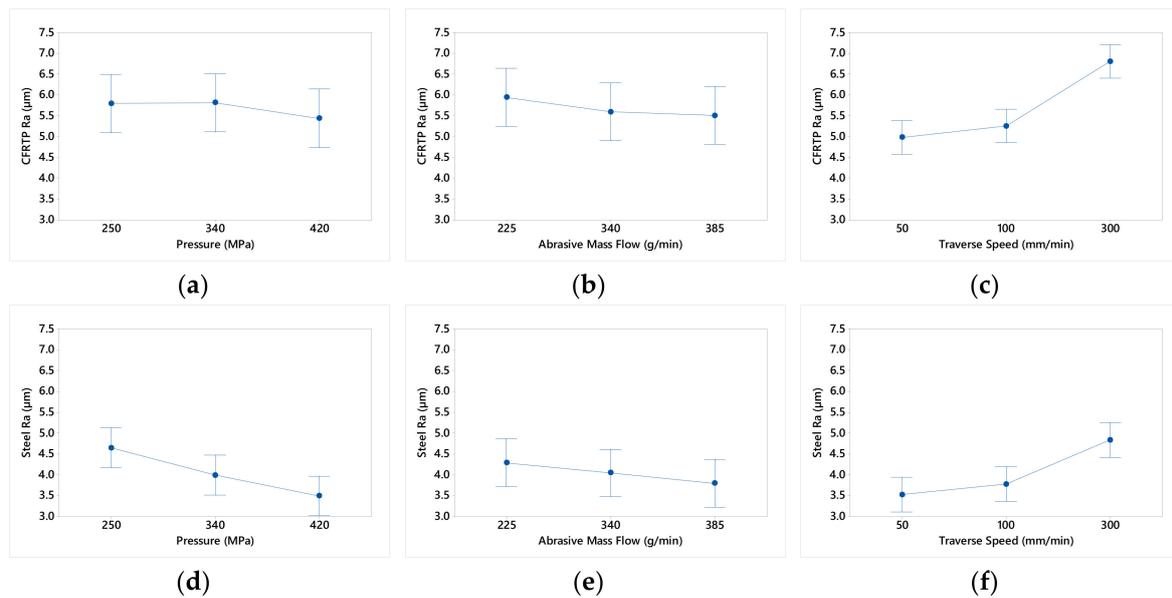
Figure 18. Cutting parameter trends in surface quality (*Ra*) in the Steel/CFRTP configuration. (**a**) CFRTP Ra in function of *P*, (**b**) CFRTP Ra in function of *AMF*, (**c**) CFRTP Ra in function of *TS*, (**d**) Steel Ra in function of *P*, (**e**) Steel Ra in function of *AMF*, and (**f**) Steel Ra in function of *TS*.
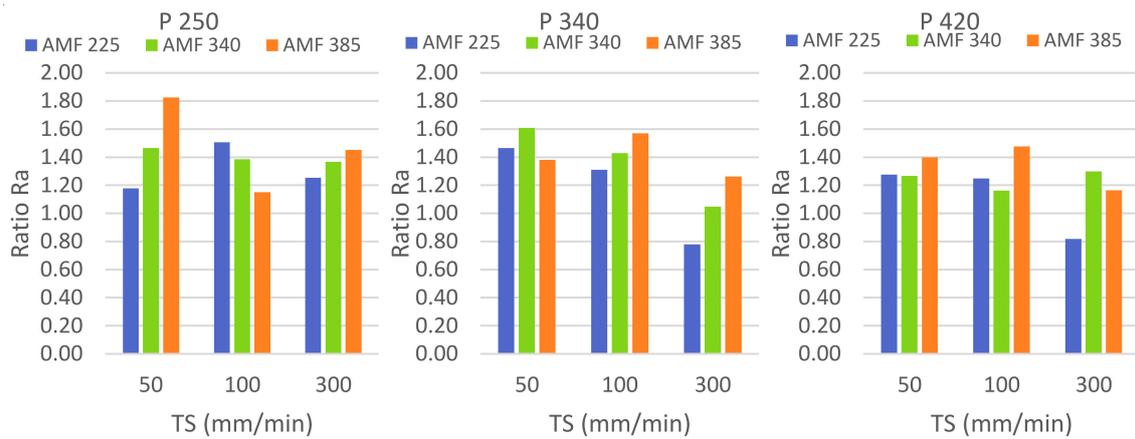

Figure 19. Ratio values *Ra* CFRTP and *Ra* Steel for CFRTP/Steel configuration.
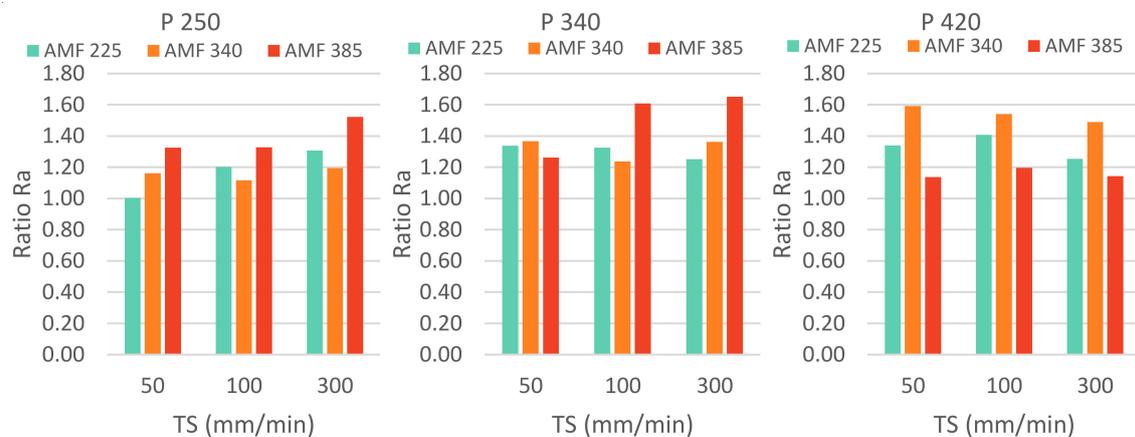

Figure 20. Ratio values *Ra* CFRTP and *Ra* Steel for Steel/CFRTP configuration.

In general, the results obtained in other studies are corroborated, where the quality obtained in the composite material is superior to steel with ratios greater than 1. In turn, in both configurations, an increase in the abrasive flow parameter produces a greater dispersion between both materials.

This can be seen especially in the CFRTP/Steel configuration, due to the fact that a greater number of abrasive particles increase the detachment of the thermoplastic matrix, causing the reinforcement to be free and worsening the surface quality. On the contrary, this increase improves the penetration capacity of the water jet allowing a stable cut in the steel and reducing the *Ra* values compared to the composite material.

It should be noted that, although the traverse speed is a parameter that worsens the surface quality considerably, its tendency is very close in both materials, which generates close ratios.

In terms of cutting parameters, ratios close to 1 are obtained for a pressure of 420 MPa because the loss of kinetic energy of the water jet is not significant, especially in the Steel/CFRTP configuration. Thus, the stacking configuration that offers the closest values of surface quality in terms of Ra is Steel/CFRTP.

It should be noted that, in both stacking configurations, gaps between materials have not been observed (Figure 21).
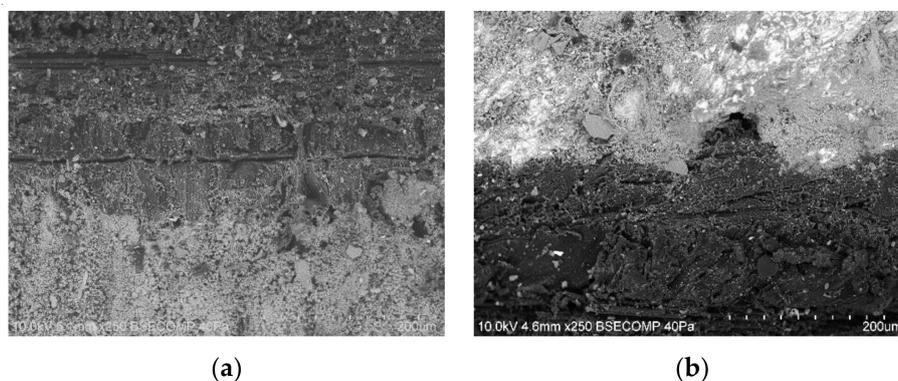

(**a**)   (**b**)

Figure 21. Final quality of the bond between materials after machining at 250× (*P* of 250 MPa, *TS* of 300 mm/min, and *AMF* of 385 g/min): (**a**) CFRTP/Steel and (**b**) Steel/CFRTP.

In both cases, abrasive particles have remained adhered to the two materials and can affect the final surface quality. In the CFRTP/Steel configuration, remains of the thermoplastic matrix can be seen that have been pulled and adhered to the surface of the steel. On the contrary, in the inverse configuration, a cleaner surface can be seen in the interlayer.

3.3. Statistical Analysis and Contour Diagrams

The percentage contribution of each cutting parameter in the surface quality for each material and stacking configuration obtained by ANOVA analysis is shown in Figure 22.

It is confirmed that the traverse speed is the most determining parameter according to the results obtained. This is particularly evident in the Steel/CFRTP configuration. An increase in this parameter generates a greater destabilization in the water jet generating a rougher surface. In addition, due to the loss of kinetic energy, the RCR region increases, leading to the formation of grooves [25,40]. On the other hand, another key factor is the hydraulic pressure. An increase in this parameter improves the penetration and machining capacity of the water jet by facilitating the removal mechanism [41].

A balance between traverse speed and hydraulic pressure has been observed in the CFRTP/Steel configuration. A correct selection of these cutting parameters reduces the hydrodistortion defect in the layers of the composite material and minimizes the detachment of the thermoplastic matrix. This results in a less rough surface and improved surface quality.
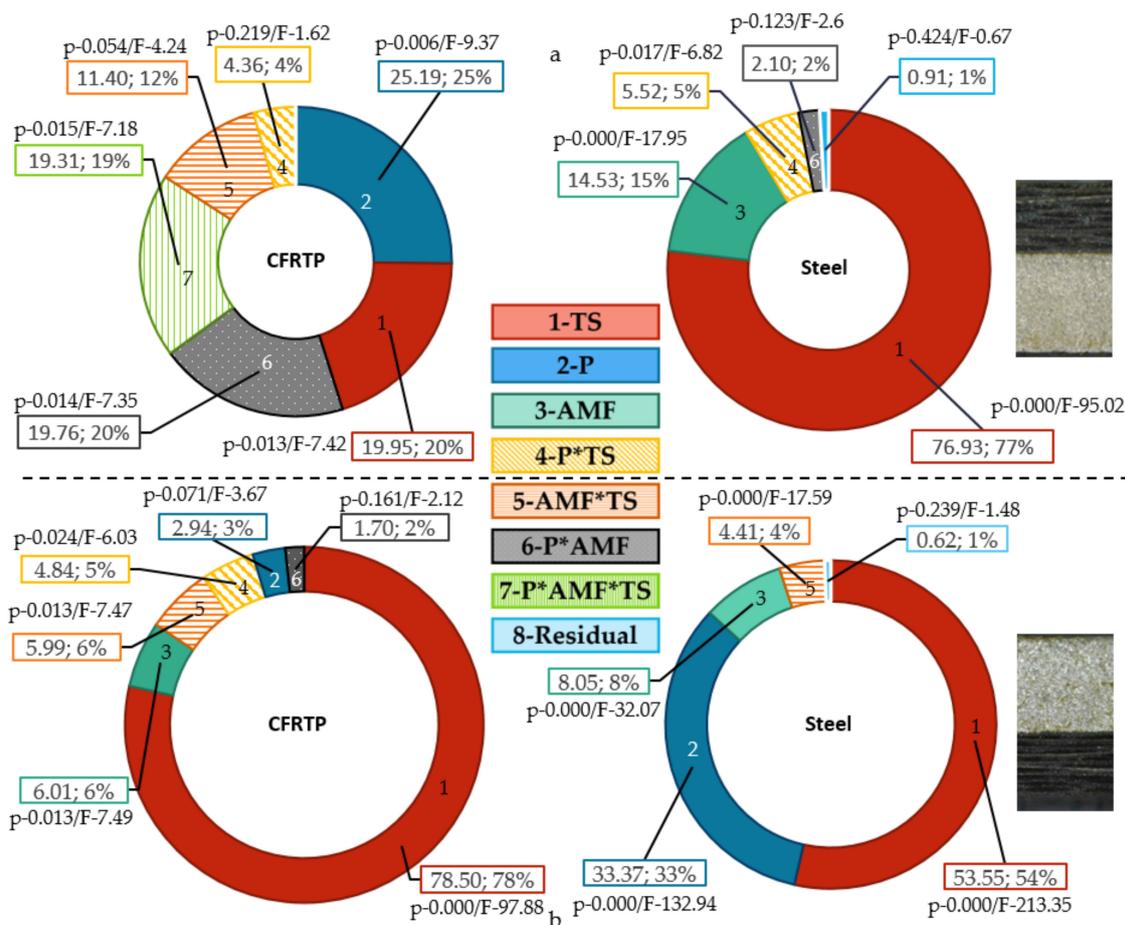
Figure 22. Percentage contribution of cutting parameters on surface quality for: (**a**) CFRTP/Steel and (**b**) Steel/CFRTP.

In parallel, with the experimental results obtained, a series of predictive second-order polynomial models have been generated that relate surface quality in terms of Ra with cutting parameters for applications in the industrial sector.

The models obtained for the CFRTP/Steel configuration are shown in (1) and (2) with values of R2 of 67.48% and 86.98%, respectively, and the models for the Steel/CFRTP configuration in (3) and (4) with adjustments of 85.73% and 95.25%, respectively. It should be noted that, due to the anisotropy and the reduced thickness of the composite material, it generates a randomness in the surface quality that reduces the adjustment obtained.

$$
\begin{aligned}
Ra\ (CFRTP) = \ & 5.37 + 0.00211{\cdot}P + 0.0050{\cdot}AMF + 0.0350{\cdot}TS - 0.000028{\cdot}P \\
& {\cdot}AMF - 0.000119{\cdot}P{\cdot}TS - 0.000123{\cdot}AMF{\cdot}TS
\end{aligned}
\tag{1}
$$

$$
\begin{aligned}
Ra\ (Steel) = \ & 6.18 - 0.00568{\cdot}P - 0.00615{\cdot}AMF + 0.0116{\cdot}TS + 0.000005{\cdot}P \\
& {\cdot}AMF - 0.000011{\cdot}P{\cdot}TS - 0.000045{\cdot}AAMF{\cdot}TS
\end{aligned}
\tag{2}
$$

$$
\begin{aligned}
Ra\ (CFRTP) = \ & -0.20 + 0.0123{\cdot}P + 0.0128{\cdot}AMF + 0.0299{\cdot}TS - 0.000032{\cdot}P \\
& {\cdot}AMF - 0.000037{\cdot}P{\cdot}TS - 0.000042{\cdot}AMF{\cdot}TS
\end{aligned}
\tag{3}
$$

$$
\begin{aligned}
Ra\ (Steel) = \ & 7.91 - 0.01441{\cdot}P - 0.00765{\cdot}AMF + 0.000025{\cdot}P{\cdot}AMF + 0.000024 \\
& {\cdot}P{\cdot}TS + 0.000003{\cdot}AMF{\cdot}TS
\end{aligned}
\tag{4}
$$

And the corresponding contour diagrams are shown in Figures 23 and 24, which relates the surface quality (*Ra*) to the cutting parameters for both stacking configurations. Values close to 4.5 μm in the

composite material in the CFRTP/Steel configuration and close to 5 µm in the Steel/CFRTP structure are obtained by combining a pressure of 420 MPa, an AMF of 385 g/min, and a *TS* of 50 mm/min in the CFRTP/Steel configuration.
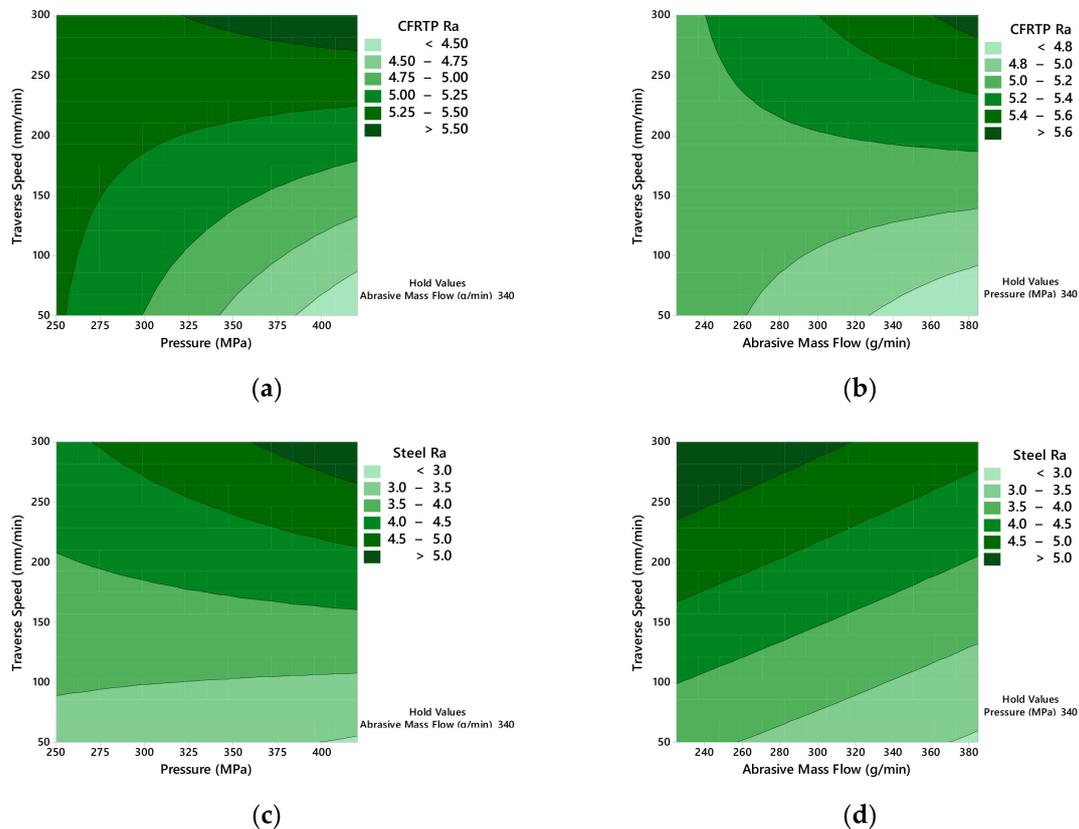

Figure 23. Contour diagrams for the CFRTP/Steel configuration: (**a**) Composite *TS* vs. *P*, (**b**) Composite *AMF* vs. *TS*, (**c**) Steel *TS* vs. *P*, and (**d**) Steel *AMF* vs. *TS*.

In this way, there is a direct relationship between the roughness generated and the ratio between the power of the water jet and the penetration depth $(\dot{E}/h)$. Very high values of this parameter indicate surfaces with low roughness. Pahuja et al. [30] explain that the composite/metal configuration shows a high initial roughness and suffers a very fast decrease in the composite material and slower in the titanium due to the loss of kinetic energy of the water jet.

Furthermore, regardless of the material, the second material to be machined suffers an increase in *Ra* values compared to the reverse configuration. Thus, it is corroborated that no matter the composite material (thermoplastic or thermoset) and the metal alloy used, the roughness in a stacked configuration is mainly governed by the characteristics of the jet. This is enhanced when the pressure is minimal due to the reduction in machining capacity.

Conversely, lower values are obtained for the metal alloy with very similar results in both stacking configurations close to 3.5 µm. These values are achieved by combining a *P* between 320 and 420 MPa, an *AMF* of 385 g/min, and a *TS* of 50 mm/min.
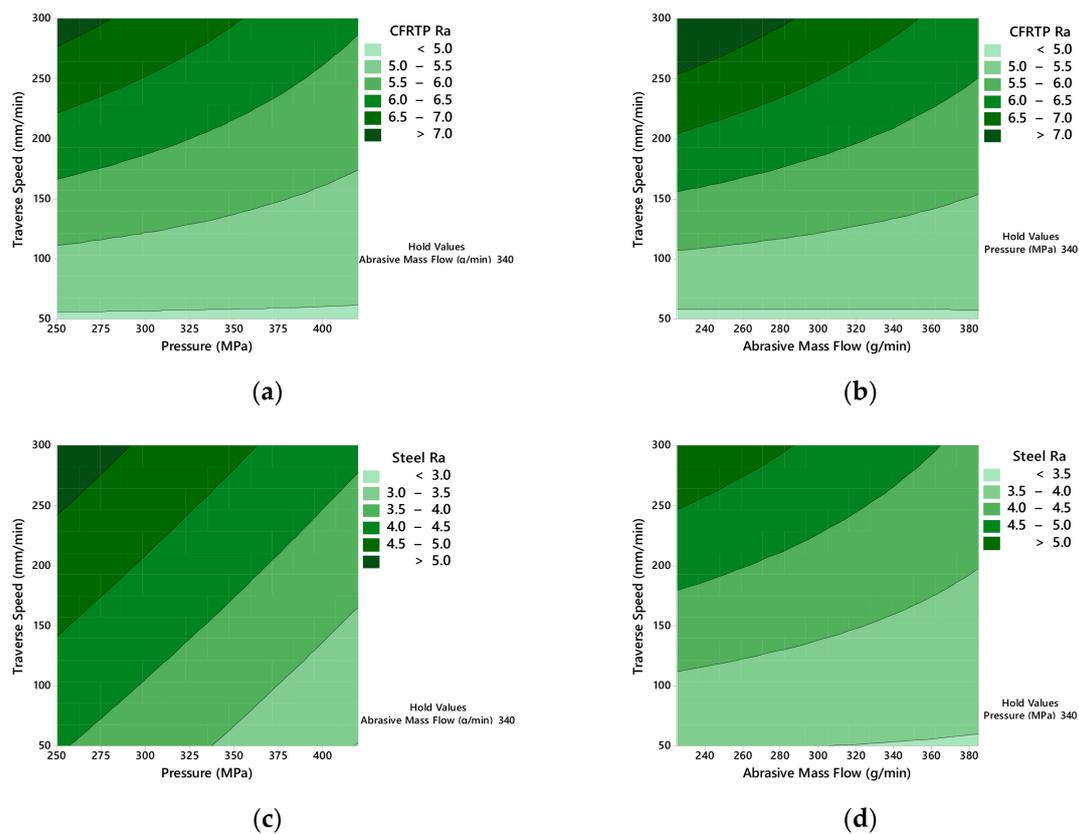
Figure 24. Contour diagrams for the Steel/CFRTP configuration: (**a**) Composite *TS* vs. *P*, (**b**) Composite *AMF* vs. *TS*, (**c**) Steel *TS* vs. *P*, and (**d**) Steel *AMF* vs. *TS*.

4. Conclusions

Surface quality in machining processes is a key parameter in terms of functional performance. Abrasive water jet machining of hybrid structures of dissimilar materials generates a highly variable surface quality that depends directly on the correct selection of cutting parameters and stacking order.

Typical defectology in abrasive water jet machining of thermoset composite materials has been identified in thermoplastic composites. Small delamination and matrix loss have been detected leaving the reinforcement unprotected.

Stacking order is a key factor. Lower *Ra* and *Rz* values are obtained in the CFRTP/Steel configuration due to better conservation of the kinetic energy of the water jet. This allows for a better cutting capacity of the water jet, especially in the composite material by minimizing matrix loss and reducing fiber pull-out defectology. In contrast, in the Steel/CFRTP configuration, due to the difference in machinability, the steel absorbs much of the energy of the water jet reducing the ability to penetrate into the composite material and resulting in a rougher and more random surface.

With regard to cutting parameters, the traverse speed is the most critical factor. In both materials and stacking configurations, an increase in this parameter generates a notable growth in the *Ra* and *Rz* values due to the divergence of the water jet and the offset that is generated between the first material and the second during machining. Thus, smoother surfaces are obtained with a traverse speed close to 50 mm/min.

The lowest values of surface quality have been obtained by combining a traverse speed of 50 mm/min, a hydraulic pressure of 420 MPa, and an abrasive mass flow of 385 g/min, maximizing the machining capacity of the water jet.

Finally, a series of predictive mathematical models have been obtained with good fits that relate the surface quality in terms of *Ra* in both materials and stacking configurations to the cutting parameters and which may be of interest and application in current industry.

Conflicts of Interest: The authors declare no conflict of interest.

Glossary of Terms

CFRTP	Carbon fiber-reinforced thermoplastics
IDR	Initial damage region
SCR	Smooth cutting region
RCR	Rough cutting region
ANOVA	Analysis of variance
P	Hydraulic pressure
AMF	Abrasive mass flow
TS	Traverse speed
AWJM	Abrasive water jet machining
TPU	Thermoplastic polyurethane

References

1. Goto, K.; Imai, K.; Arai, M.; Ishikawa, T. Shear and tensile joint strengths of carbon fiber-reinforced thermoplastics using ultrasonic welding. *Compos. Part A Appl. Sci. Manuf.* **2019**, *116*, 126–137. [CrossRef]

2. Ishikawa, T.; Amaoka, K.; Masubuchi, Y.; Yamamoto, T.; Yamanaka, A.; Arai, M.; Takahashi, J. Overview of automotive structural composites technology developments in Japan. *Compos. Sci. Technol.* **2018**, *155*, 221–246. [CrossRef]

3. Christmann, M.; Medina, L.; Mitschang, P. Effect of inhomogeneous temperature distribution on the impregnation process of the continuous compression molding technology. *J. Thermoplast. Compos. Mater.* **2017**, *30*, 1285–1302. [CrossRef]

4. Biron, M. Outline of the actual situation of plastics compared to conventional materials. In *Thermoplastics and Thermoplastic Composites*; William Andrew: Norwich, NY, USA, 2018; Volume i, pp. 1–32, ISBN 9780081025017.

5. Bu, H.; Li, Y.; Yang, H.; Wang, L.; Zhan, X. Investigation of laser joining process of CFRTP and aluminum alloy. *Mater. Manuf. Process.* **2020**, 1–8. [CrossRef]

6. Haider, D.R.; Krahl, M.; Liebsch, A.; Kupfer, R.; Haider, D.R.; Krahl, M.; Koshukow, W.; Wolf, M.; Liebsch, A.; Kupfer, R.; et al. Adhesion Studies of Thermoplastic Fibre-Plastic Composite Hybrid Components Part 2: Thermoplastic-Metal-Composites. In Proceedings of the Hybrid Materials and Structures 2018, Bremen, Germany, 18–19 April 2018.

7. Sheng, L.; Jiao, J.; Du, B.; Wang, F.; Wang, Q. Influence of Processing Parameters on Laser Direct Joining of CFRTP and Stainless Steel. *Adv. Mater. Sci. Eng.* **2018**, *2018*, 1–15. [CrossRef]

8. Sheng, L.Y.; Wang, F.Y.; Wang, Q.; Jiao, J.K. Shear Strength Optimization of Laser-Joined Polyphenylene Sulfide-Based CFRTP and Stainless Steel. *Strength Mater.* **2018**, *50*, 824–831. [CrossRef]

9. Jiao, J.; Xu, Z.; Wang, Q.; Sheng, L.; Zhang, W. CFRTP and stainless steel laser joining: Thermal defects analysis and joining parameters optimization. *Opt. Laser Technol.* **2018**, *103*, 170–176. [CrossRef]

10. Mamalis, D.; Obande, W.; Koutsos, V.; Blackford, J.R.; Ó Brádaigh, C.M.; Ray, D. Novel thermoplastic fibre-metal laminates manufactured by vacuum resin infusion: The effect of surface treatments on interfacial bonding. *Mater. Des.* **2019**, *162*, 331–344. [CrossRef]

11. Tanaka, K.; Yamashiro, T.; Katayama, T. Internal Damage Evaluation of Cfrtp Cut By a Circular Saw. *Mater. Contact Charact.* **2017**, *116*, 345–351.

12. Masek, P.; Zeman, P.; Kolar, P. Development of a Cutting Tool for Composites With Thermoplastic Matrix. *Sci. J.* **2013**, 423–427. [CrossRef]

13. Kakinuma, Y.; Ishida, T.; Koike, R.; Klemme, H.; Denkena, B.; Aoyama, T. Ultrafast Feed Drilling of Carbon Fiber-Reinforced Thermoplastics. *Procedia CIRP* **2015**, *35*, 91–95. [CrossRef]

14. Zitoune, R.; Krishnaraj, V.; Collombet, F. Study of drilling of composite material and aluminium stack. *Compos. Struct.* **2010**, *92*, 1246–1255. [CrossRef]

15. Bañon, F.; Sambruno, A.; Batista, M.; Simonet, B.; Salguero, J. Study of the surface quality of carbon fiber–reinforced thermoplastic matrix composite (CFRTP) machined by abrasive water jet (AWJM). *Int. J. Adv. Manuf. Technol.* **2020**, *107*, 3299–3313. [CrossRef]

16. Ramulu, M.; Pahuja, R.; Hashish, M.; Isvilonanda, V. Abrasive Waterjet Machining Effects on Kerf Quality in Thin Fiber Metal Laminate. In Proceedings of the WJTA-IMCA Conference and Expo, New Orleans, LA, USA, 2–4 November.

17. El-Hofy, M.; Helmy, M.O.; Escobar-Palafox, G.; Kerrigan, K.; Scaife, R.; El-Hofy, H. Abrasive Water Jet Machining of Multidirectional CFRP Laminates. *Procedia CIRP* **2018**, *68*, 535–540. [CrossRef]

18. Perec, A. Environmental aspects of abrasive water jet cutting. *Rocz. Ochr. Sr.* **2018**, *20*, 258–274.

19. Pahuja, R.; Ramulu, M. Abrasive water jet machining of Titanium (Ti6Al4V)–CFRP stacks – A semi-analytical modeling approach in the prediction of kerf geometry. *J. Manuf. Process.* **2019**, *39*, 327–337. [CrossRef]

20. Pahuja, R.; Ramulu, M.; Hashish, M. Abrasive Water jet machining (AWJ) of hybrid Titanium/Graphite composite laminate: Preliminary results. In Proceedings of the 22nd International Conference on Water Jetting, Haarlem, The Netherlands, 3–5 September 2014; pp. 83–95.

21. Pahuja, R.; Ramulu, M.; Hashish, M. Abrasive waterjet profile cutting of thick Titanium/Graphite fiber metal laminate. In *ASME International Mechanical Engineering Congress and Exposition*; American Society of Mechanical Engineers: New York, NY, USA, 2016; pp. 1–11.

22. Li, M.; Huang, M.; Chen, Y.; Gong, P.; Yang, X. Effects of processing parameters on kerf characteristics and surface integrity following abrasive waterjet slotting of Ti6Al4V / CFRP stacks. *J. Manuf. Process.* **2019**, *42*, 82–95. [CrossRef]

23. Alberdi, A.; Artaza, T.; Suárez, A.; Rivero, A.; Girot, F. An experimental study on abrasive waterjet cutting of CFRP/Ti6Al4V stacks for drilling operations. *Int. J. Adv. Manuf. Technol.* **2016**, *86*, 691–704. [CrossRef]

24. Sambruno, A.; Bañon, F.; Salguero, J.; Simonet, B.; Batista, M. Kerf Taper Defect Minimization Based on Abrasive Waterjet Machining of Low Thickness Thermoplastic Carbon Fiber Composites C/TPU. *Materials* **2019**, *12*, 4192. [CrossRef]

25. Dumbhare, P.A.; Dubey, S.; Deshpande, Y.V.; Andhare, A.B.; Barve, P.S. Modelling and multi-objective optimization of surface roughness and kerf taper angle in abrasive water jet machining of steel. *J. Braz. Soc. Mech. Sci. Eng.* **2018**, *40*, 259. [CrossRef]

26. Ruiz-Garcia, R.; Mayuet Ares, P.; Vazquez-Martinez, J.; Salguero Gómez, J. Influence of Abrasive Waterjet Parameters on the Cutting and Drilling of CFRP/UNS A97075 and UNS A97075/CFRP Stacks. *Materials* **2018**, *12*, 107. [CrossRef] [PubMed]

27. Bañon, F.; Sambruno, A.; Ruiz-Garcia, R.; Salguero, J.; Mayuet, P.F. Study of the influence of cutting parameters on surface quality in AWJM machining of thermoplastic matrix composites. *Procedia Manuf.* **2019**, *41*, 233–240. [CrossRef]

28. Mayuet Ares, P.F.; Rodríguez-Parada, L.; Gómez-Parra, A.; Batista, M. Characterization and Defect Analysis of Machined Regions in Al-SiC Metal Matrix Composites Using an Abrasive Water Jet Machining Process. *Appl. Sci.* **2020**, *10*, 1512. [CrossRef]

29. Zhang, S.; Ji, L.; Wu, Y.; Chen, M.; Zhou, W. Exploring a new method to obtain the 3D abrasive water jet profile. *Int. J. Adv. Manuf. Technol.* **2020**, 4797–4809. [CrossRef]

30. Pahuja, R.; Ramulu, M.; Hashish, M. Surface quality and kerf width prediction in abrasive water jet machining of metal-composite stacks. *Compos. Part B Eng.* **2019**, *175*, 107134. [CrossRef]

31. Chithirai, M.; Selvan, P.; Mohana, N.; Raju, S. Assessment of Process Parameters in Abrasive Waterjet Cutting of Stainless Steel. *Int. J. Adv. Eng. Technol.* **2011**, *1*, 34.

32. Bañon, F.; Sambruno, A.; Batista, M.; Simonet, B.; Salguero, J. Surface Quality and Free Energy Evaluation of s275 Steel by Shot Blasting, Abrasive Water Jet Texturing and Laser Surface Texturing. *Metals* **2020**, *10*, 290.

33. Mathia, T.G.; Pawlus, P.; Wieczorowski, M. Recent trends in surface metrology. *Wear* **2011**, *271*, 494–508. [CrossRef]

34. Masek, P.; Kolar, P.; Zeman, P. Optimization of trimming operations for machining carbon fibre reinforced thermoplastic composite. In Proceedings of the International Conference on Advanced Manufacturing Engineering and Technologies (NEWTECH 2013), Stockholm, Sweden, 27–30 October 2013. Available online: https://www.researchgate.net/publication/272576514_Optimization_of_trimming_operations_for_machining_carbon_fibre_reinforced_thermoplastic_composite (accessed on 23 June 2020).

35. Mayuet Ares, P.F.; Girot Mata, F.; Batista Ponce, M.; Salguero Gñmez, J. Defect Analysis and Detection of Cutting Regions in CFRP Machining Using AWJM. *Materials* **2019**, *12*, 4055. [CrossRef]

36. Pahuja, R.; Ramulu, M. Surface quality monitoring in abrasive water jet machining of Ti6Al4V–CFRP stacks through wavelet packet analysis of acoustic emission signals. *Int. J. Adv. Manuf. Technol.* 2019. Available online: https://www.researchgate.net/publication/334756766_Surface_quality_monitoring_in_abrasive_water_jet_machining_of_Ti6Al4V-CFRP_stacks_through_wavelet_packet_analysis_of_acoustic_emission_signals (accessed on 23 June 2020).

37. Kumar, S.; Laxminarayana, P. Optimization of Process Parameters on Kerf Width & Taper Angle on En-8 Carbon Steel by Abrasive Water Jet Machining. Available online: https://www.researchgate.net/publication/332171967_Optimization_of_Process_Parameters_on_Kerf_Width_Taper_Angle_on_En-8_Carbon_Steel_by_Abrasive_Water_Jet_Machining (accessed on 23 June 2020).

38. Chithirai, M.; Selvan, P.; Mohana, N.; Raju, S. A Machinability Study of Kevlar-Phenolic Composites Using Abrasive Waterjet Cutting Process. *CLEAR IJRET* **2012**, *1*, 46–57. Available online: https://www.semanticscholar.org/paper/A-Machinability-Study-of-Kevlar-Phenolic-Composites-Selvan-Raju/18f1f090fd279616eb814562f177db664b5461ca (accessed on 23 June 2020).

39. Köhler, T.; Röding, T.; Gries, T.; Seide, G. An Overview of Impregnation Methods for Carbon Fibre Reinforced Thermoplastics. *Key Eng. Mater.* **2017**, *742*, 473–481. [CrossRef]

40. Rao, M.S. Parametric Optimization of Abrasive Waterjet Machining for Mild Steel: Taguchi Approach. *Int. J. Curr. Eng. Technol.* **2014**, *2*, 28–30. [CrossRef]

41. Murugabaaji, V.; Kannan, A.; Nagarajan, N. Experimental Investigation on Abrasive Waterjet Machining of Stainless Steel 304. 2015. Available online: https://www.researchgate.net/publication/330577552_Experimental_Investigation_on_Abrasive_Waterjet_Machining_of_Stainless_Steel_304 (accessed on 23 June 2020).